Defect and Diffusion Forum
ISSN: 1662-9507, Vol. 451, pp 87-94
doi:10.4028/p-c6k3HY

Submitted: 2026-01-12
Revised: 2026-03-02
Accepted: 2026-03-03
Online: 2026-04-17

Meshless Transient Thermal Modeling of Polymer Composite Curing with Exothermic Heat Generation

TOSI Igor F.[1,a*], PEDRUZZI Wancley O.[,2,b], QUIROZ William P. M.[,4,c], D'ELIA Raffaele[,5,d], DUTRA Julio C. S.[,3,e], and DA SILVA Wellington B.[3,f]

[1]Graduate Program in Chemical Engineering, Universidade Federal do Espírito Santo, Brazil

[2]Graduate Program of Mechanical Engineering, Universidade Federal do Espírito Santo, Brazil.

[3]Department of Rural Engineering, Universidade Federal do Espírito Santo, Brazil.

[4]Universidad San Sebastián, Campus Bellavista, Chile.

[5]Institut Clément Ader (ICA), Univ Toulouse, IMT Mines Albi, INSA Toulouse, ISAE Sup Aero, CNRS, ICA, Albi France.

[a] igor.tosi@edu.ufes.br , [b]wancley.pedruzzi@edu.ufes.br, [c]william.montes@uss.cl, [d]raffaele.delia@mines-albi.fr, [e]julio.dutra@ufes.br, [f]wellingtonufes@gmail.com

Keywords: Method of Fundamental Solutions, Method of Particular Solutions, Meshless Method, composite

Abstract. This work presents a hybrid formulation combining the Method of Fundamental Solutions (MFS) and the Method of Particular Solutions (MPS) coupled with an implicit Finite Difference Method (FDM) to simulate the transient heat conduction in a two-layer domain composed of a steel tool and an epoxy resin. The proposed approach incorporates a non-homogeneous source term in the governing equation, allowing the analysis of the curing heat release within the resin layer while maintaining a meshless boundary-based structure. Sequential numerical tests were performed to empirically assess the influence of key hyper-parameters number and position of source points, distance parameters, and the Tikhonov regularization factor on the stability and accuracy of the method. The MFS-MPS/FDM model showed excellent agreement with the finite element results reported by Dei Sommi et al., achieving low RMSE (Root Mean Squared Error) and MAE (Mean Absolute Error) values relative to the thermal scale of the process. These results confirm the robustness and predictive capability of the MFS in capturing transient thermal evolution even in the presence of a source term, although its performance remains sensitive to the proper calibration of numerical hyper-parameters.

Introduction

When subjecting a laminated composite to an autoclave curing process, it is essential to closely monitor the thermodynamic conditions imposed on the evaluated material. Under certain circumstances, the undesirable formation of voids (pores) may occur. High initial moisture levels and lower autoclave pressure contributed to the emergence of voids on the tool side, where the residual water concentration is typically higher [1]. The relationship between the initial amount of moisture absorbed by the resin and the hydrostatic pressure during curing was also investigated by [2], combining the theoretical modeling of Kardos and Ledru with experimental tests and computational numerical analysis using the Finite Element Method (FEM).

Computational numerical models serve as essential tools for investigating the parameters that contribute to pore formation in materials, offering viable alternatives to experimental routines. Established methods such as the FEM, the Finite Volume Method (FVM), and the FDM have been widely applied in the simulation of complex physical phenomena in composites, such as heat diffusion and mechanical strength [3, 4].

In this context, meshless methods represent an approach that eliminates the need for discretizing the domain into a continuous mesh, leading to a significant reduction in computational cost while also enhancing the flexibility in modeling complex geometries. Among these methodologies, the MFS

stands out due to its consistent numerical formulation, making it particularly suitable for the analysis of layered media and applications involving heat transfer in laminated materials [5]. However, for the application of this technique, knowledge of the fundamental solution of the partial differential equation (PDE) is crucial, as it is restricted to homogeneous PDEs. The presence of the source term in the equation precludes the application of the MFS in its classical form, necessitating its decomposition into homogeneous and particular components [6].

The MPS can be naturally integrated with the Method of Fundamental Solutions (MFS), enabling the treatment of non-homogeneous terms through auxiliary approximations such as Radial Basis Functions (RBF) or Finite Difference schemes [7, 8]. Previous applications of the MFS in composite materials have been predominantly restricted to elliptic, Helmholtz-type problems, where the non-homogeneous term is transformed into combinations of RBFs in order to convert the governing equation into an equivalent homogeneous system [9]. Such formulations, however, are typically limited to steady-state or non-transient settings.

In contrast, the present study introduces a fully transient and nonlinear meshless formulation of heat conduction in a multilayer domain, in which the governing PDE contains a time-dependent, temperature-dependent volumetric source term. The proposed framework unifies the MFS with the MPS-FDM approach in a hybrid strategy that preserves the meshless character of the MFS while consistently incorporating the non-homogeneous and nonlinear contributions into the transient evolution of the solution.

Unlike previous approaches that rely on spatial discretization or stationary reformulations, the proposed method directly handles the time-dependent non-homogeneous term without requiring domain meshing, enabling efficient simulation of coupled thermo-reactive phenomena in layered materials. This represents a significant methodological advancement, extending the MFS from classical elliptic applications to a robust transient formulation capable of addressing nonlinear heat conduction in composite multi-domain systems.

Methodology

The methodology implemented in this work is based on the numerical solution of a thermal model coupled with transport-related quantities, aimed at assessing the influence of temperature on pressure and on the mass diffusion coefficient D. The temperature field is treated as the primary variable of the entire model and is obtained from the transient heat conduction equation. Based on this field, temperature-dependent quantities are updated and used to evaluate the pressure, which in turn influences diffusion-related phenomena. Consequently, the diffusion coefficient is not treated as a constant at each iteration, but rather as a variable quantity, consistently determined according to the thermal state of the system.

Thermal Model

The transient thermal model, represents the state to be determined at each time iteration, where $\Psi(t)$ denotes the source term associated with the degree of cure of the material.

$$u_t = \alpha \nabla^2 u_{xx} + \Psi(t) \tag{1}$$

In order to achieve accurate results while maintaining low computational cost, a meshless method is adopted, thereby avoiding the discretization of the physical domain. Accordingly, the MFS is employed to analyze the transient thermal behavior of a homogeneous model by associating the fundamental solution also referred to as the Green's function of the heat conduction PDE. However, since Eq. (1) includes a source term, the direct application of the MFS is not possible, requiring its coupled use with an auxiliary methodology for the approximation of $\Psi(t)$.

$$u_G(x,t) = u_H(x,t) + \tilde{u}(x,t) \tag{2}$$

Thus, based on the MPS, the solution of the non-homogeneous heat conduction PDE is decomposed into the sum of a homogeneous solution, $u_H(x,t)$, obtained via the MFS, and a particular solution,$\tilde{u}(x,t)$, computed using the FDM as expressed in Eq.(2).

Formulation of the MFS for the Homogenuos Heat Equation

The MFS approximates the solution of the homogeneous heat conduction PDE through linear combinations of fundamental solutions, allowing the problem to be solved without discretizing the physical domain. This approach relies solely on collocation points located on the boundary and source points placed in a region external to the physical domain.

$$G(x,t;\xi,\tau) = \frac{H(t-\tau)}{\sqrt{4\pi\alpha(t-\tau)}} \exp\left(-\frac{(x-\xi)^2}{4\alpha(t-\tau)}\right) \tag{3}$$

Equation (3) represents the fundamental solution of Eq. (1) for $\Psi(t) = 0$, where x denotes the collocation points and ξ the source points. The temporal source points τ are introduced such that $\tau = t - \Delta t$. The function $H(t-\tau)$ corresponds to the Heaviside step function, ensuring that the fundamental solution vanishes for $t < \tau$. A linear system is then constructed from the fundamental solutions together with the boundary and initial conditions, where c denotes the vector of coefficients to be determined from the inclusion of N_s sources.

$$u_H(x,t) \approx \sum_{j=1}^{N_s} c_j \, G(x,t;\xi_j,\tau_j) \tag{4}$$

However, the fundamental solution matrix computed in Eq. (3) requires regularization prior to solving the system, as it exhibits strongly linearly dependent columns as well as highly singular values. Therefore, Tikhonov regularization is applied by introducing a small-order penalty parameter λ:

$$(\mathbf{A}^T\mathbf{A} + \lambda^2\mathbf{I})\, c = \mathbf{A}^T b \tag{5}$$

Equation (5) illustrates the system composed of the fundamental solution matrix (**A**), the identity matrix (**I**), the boundary conditions vector (b), and the vector of unknown coefficients (c).

Particular Solution and Coupling with the MFS

Due to the inherent limitations of the MFS, the MPS is employed as an auxiliary strategy to approximate the source term $\Psi(t)$, transferring its effect to the boundary conditions of the problem solved by the MFS. Accordingly, the boundary vector (b) is updated at each time iteration as a result of the influence of the degree of cure on the system.

$$\frac{u_i^{n+1} - u_i^n}{\Delta t} = \alpha \frac{\tilde{u}_{i+1}^{n+1} - 2\tilde{u}_i^{n+1} + \tilde{u}_{i-1}^{n+1}}{\Delta x^2} + \Psi(t_{n+1}) \tag{6}$$

An implicit time integration scheme is adopted for the evaluation of the degree of cure, which is subsequently incorporated into the homogeneous model solved using the MFS. Equation (6) describes the finite difference scheme employed to compute the particular solution introduced in Eq. (2), while Eq. (7) defines the homogeneous boundary conditions imposed within the MPS framework.

$$\begin{cases} h\tilde{u}(x_0,t) - k\dfrac{\partial\tilde{u}(x_0,t)}{\partial n} = 0 \\ h\tilde{u}(x_L,t) + k\dfrac{\partial\tilde{u}(x_L,t)}{\partial n} = 0 \end{cases} \tag{7}$$

General Solution

The general solution of the governing PDE is obtained through an iterative MFS-MPS scheme, in which the source term $\Psi(t)$ is treated exclusively by the MPS. This approach generates a correction term that is incorporated into the boundary conditions of the MFS. As a result, the problem is homogenized, enabling the reconstruction of the temperature field through a linear combination of the fundamental solutions of the heat conduction equation.

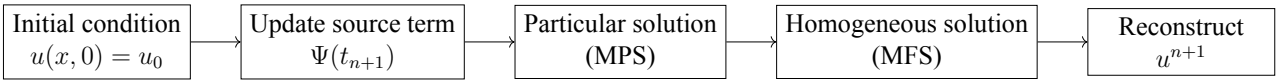

Fig. 1: Iterative MFS–MPS computational scheme.

Water vapor pressure is calculated locally as a function of temperature, following [1, 2], as given in Eq. (8). At each time step, the temperature field provided by the MFS-MPS thermal model is used to update the vapor pressure values.

$$P_{\text{water}} = 611.21 \ \exp\left(\frac{18.678\,u}{234.5}\right)\left(\frac{u}{257.14+u}\right) \tag{8}$$

No spatial pressure gradients or transport mechanisms are considered, and the pressure is evaluated solely as a function of the local temperature. Likewise, the diffusion coefficient is investigated as a temperature-dependent parameter, without the need to solve the mass diffusion governing equation. Its temporal evolution reflects the effect of temperature on the mobility of volatile species within the material and is updated at each time step using an Arrhenius-type formulation:

$$D(u) = D_0 \exp\left(-E_{ad}/Ru\right) \tag{9}$$

Error Metrics

The tests for the MFS were conducted sequentially, empirically evaluating the influence of each hyperparameter on the final results. The method's ability to capture the thermal evolution was quantitatively assessed using the RMSE and MAE error metrics, which measure the discrepancy between the numerical results and the reference model, as shown in Eq. (10).

$$\text{RMSE} = \sqrt{\frac{1}{N}\sum_{i=1}^{N}\left(u_i^{\text{num}} - u_i^{\text{ref}}\right)^2} \qquad \text{MAE} = \frac{1}{N}\sum_{i=1}^{N}\left|u_i^{\text{num}} - u_i^{\text{ref}}\right| \tag{10}$$

Physical Problem

The domains are coupled at Γ_{12}, Figure 2, with perfect thermal contact between the layers. In the resin domain,P a source term $\Psi(t)$ is present, associated with the exothermic curing reaction process, modeled by:

$$\Psi(t) = \kappa_1(\alpha_{\text{max}} - \alpha)^{n_1} + \kappa_2(\alpha_{\text{max}} - \alpha)^{n_2} \qquad \alpha_{\text{max}} = p + qu \tag{11}$$

The kinetic constants κ_1 and κ_2 are updated at each iteration, as they depend directly on the temperature, according to the Arrhenius relation:

$$\kappa_j = k_{0j} \exp\left(-E_{a_j}/Ru\right) \qquad j = 1, 2 \tag{12}$$

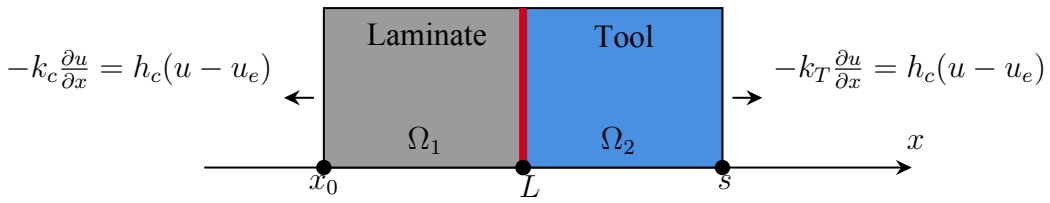

Fig. 2: Sketch of the model domain, where L and s are the laminate and tool thickness, respectively.

The thermal problem is defined over a one-dimensional composite domain $\Omega = [0, L + s]$, composed of the resin region ($0 \leq x \leq L$) and the tool region ($L < x \leq L + s$). The governing equations read:

$$\begin{cases} \rho_c c_{pc} \dfrac{\partial u}{\partial t} = k_c \dfrac{\partial^2 u}{\partial x^2} + \rho_c \Delta h_{ref} \Psi(t), & 0 \leq x \leq L, \\ \rho_t c_{pt} \dfrac{\partial u}{\partial t} = k_t \dfrac{\partial^2 u}{\partial x^2}, & L < x \leq L + s. \end{cases} \tag{13}$$

The initial condition is prescribed as $u(x, 0) = u_0,\ x \in \Omega$. Convective boundary conditions are imposed at both external surfaces in $x = x_0$ and $x = L + s$. The autoclave temperature $u_e(t)$ varies linearly in time, imposing a controlled heating rate $\dot{u} = 2°\text{C/min}$ from the initial temperature u_0:

$$u_e(t) = u_0 + \dot{u}\, t. \tag{14}$$

Table 1: Parameters used in the thermal and kinetic model of the test case

Symbol	Value	Unit	Symbol	Value	Unit
m	5.80×10^{-1}	–	n_1	7.90×10^{-1}	–
n_2	1.99	–	k_{01}	1.15×10^{10}	s^{-1}
k_{02}	1.40×10^{2}	s^{-1}	E_{a1}	1.27×10^{5}	J/mol
E_{a2}	4.51×10^{4}	J/mol	Δh	3.56×10^{5}	J/kg
R	8.314	J/mol	p	-2.54	–
q	7.4×10^{-3}	K^{-1}	ρ_c	1.58×10^{3}	kg/m^3
c_{pc}	8.71×10^{2}	$J/(kg \cdot K)$	k_c	0.43	$W/(mK)$
ρ_t	2.7×10^{3}	kg/m^3	c_{pt}	9×10^{2}	$J/(kg \cdot K)$
k_t	1.45×10^{2}	$W/(mK)$	L	5.58	mm
s	20	mm	h	40	$W/(m^2K)$
u_0	20	$°C$	$u_{\max}$	180	$°C$

Results and Discussion

The tests for the MFS were conducted sequentially, empirically evaluating the influence of each hyperparameter on the final results, according to the input parameters showing in Tab. 1. The Tab 2 shows that the computational algorithm proposed in this work exhibits excellent agreement with the results of [1], considering that the RMSE and MAE errors are within acceptable levels ≈ 0.1 relative to the temperature scale.

Table 2: Error indicators and computational cost for different numerical configurations.

N_t	N_x	N_s	δ_1	δ_2	λ	Midplane – $L/2$		Tool side		CPU (s)
						RMSE	MAE	RMSE	MAE	
60	120	480	1	1.32	1×10^{-11}	0.1128	0.0940	0.0116	0.0158	21.411
60	120	480	1	1.35	5×10^{-11}	0.1052	0.0850	0.0116	0.0158	22.875
60	120	480	1	1.50	1×10^{-12}	0.0916	0.0675	0.0328	0.0279	21.290
30	60	240	1	1.00	1×10^{-8}	0.0562	0.0432	0.0122	0.0163	4.127
22	44	176	1	1.00	1×10^{-10}	0.0928	0.1130	0.0234	0.0190	3.313
18	36	144	1	1.00	9×10^{-5}	0.0556	0.0463	0.0116	0.0159	3.283

Moreover, Table 2 shows that the errors are closely linked to the space-time discretization, as well as to the calibration of the parameters δ_1, δ_2, and λ, which represents an inherent challenge of the proposed method. Increasing the number of collocation points N_x and fictitious sources N_s contributes to the reduction of RMSE and MAE errors, reflecting the model's convergence with respect to refinement.

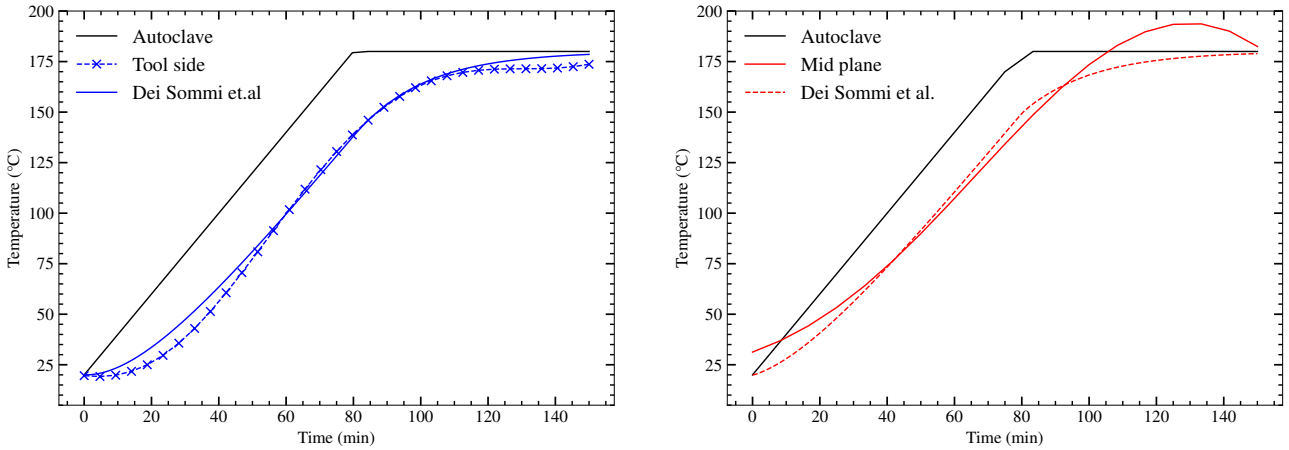

(a) Tool Side (b) Mid Plane

Fig. 3: Time dependence of temperature in tool side and mid plane respectively

The laminate temperature exceeding the autoclave temperature, particularly at the mid-plane, is physically consistent with the exothermic curing of the epoxy resin. The volumetric heat source term $\Psi(t)$ represents the heat released during polymerization. At the peak reaction rate, the internally generated heat may exceed the heat removed by convection, leading to thermal accumulation at the mid-plane which is more insulated and has higher thermal inertia and resulting in a temperature overshoot. This behavior is commonly reported in thermoset curing simulations and arises from the coupled thermo-kinetic nature of the process rather than from a numerical artifact.

On the other hand, the displacement of the source points exhibits a markedly nonlinear influence on the MFS performance. Very small displacements tend to deteriorate the conditioning of the fundamental solution matrix, whereas excessively large displacements reduce the accuracy of the temperature field near the boundaries. The regularization parameter λ also plays a crucial role in the MFS, as it controls numerical noise and ensures stability in the computation of the coefficient vector c.

As observed in Fig. 3, larger deviations are detected in the mid-plane region of the laminate. This behavior is attributed to the thermal inertia of the resin, which delays the temperature response and its subsequent stabilization, particularly after the $180°$C plateau. In contrast, at the tool surface where the thermal flux is more intense the MFS reproduces the reference solution with higher accuracy.

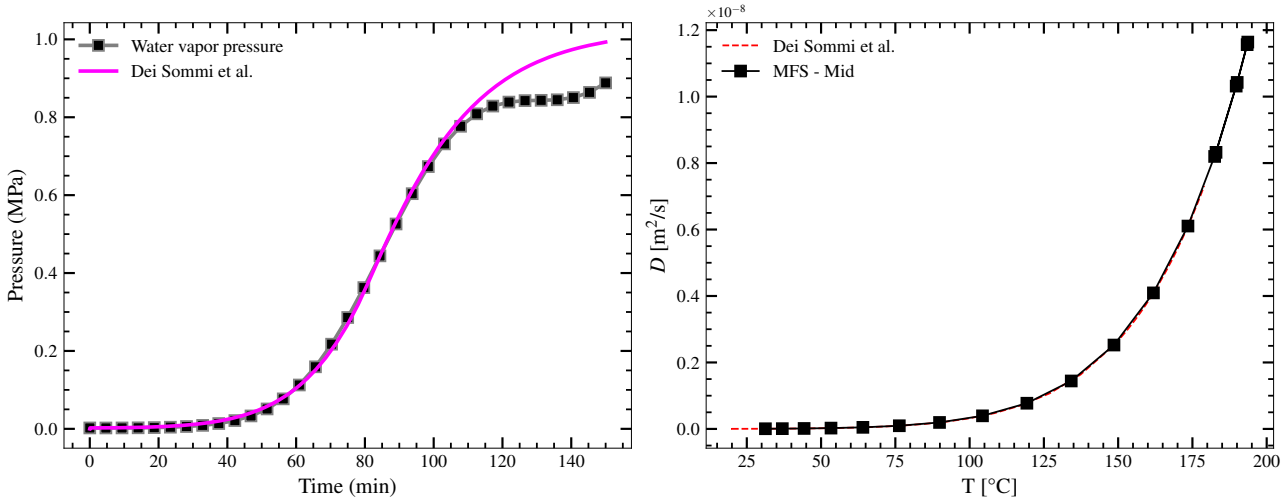

Fig. 4: Comparison between the simulated water vapor pressure and the experimental data reported by Dei Sommi et al. as a function of time. (Right) Temperature-dependent diffusivity obtained from the FEM and MFS models at the mid-plane position.

Figure 4 presents the evolution of the water vapor pressure and the temperature-dependent diffusion coefficient obtained using the proposed MFS–MPS framework. In the left panel, the simulated vapor pressure exhibits excellent agreement with the experimental data reported by Dei Sommi et al., yielding an RMSE of 0.0495 and an MAE of 0.0287. This close agreement confirms that the thermal model accurately captures the dominant thermally driven mechanism governing vapor pressure evolution during curing. The predicted pressure curve displays a characteristic sigmoidal behavior, with an initially slow increase followed by a rapid rise after approximately 60 minutes. This transition coincides with the temperature range in which moisture vaporization becomes significant, indicating that the computed water vapor pressure is physically consistent with the curing cycle and the associated thermal history. The accurate reproduction of this trend is particularly relevant, as elevated vapor pressure constitutes the primary driving force for void nucleation and growth during curing.

The right panel depicts the diffusion coefficient as a function of temperature evaluated at the laminate mid-plane. The MFS-based thermal field closely follows the Arrhenius-type behavior reported in the reference study, demonstrating that the proposed framework correctly captures the exponential sensitivity of diffusivity to temperature. The combined evolution of P_{water} and $D(u)$ highlights competing mechanisms during curing. While the rapid increase in vapor pressure promotes gas expansion and elevates the risk of porosity formation, the simultaneous increase in diffusivity enhances the mobility of volatile species, potentially facilitating their redistribution or release when transport pathways are available. Therefore, even without explicitly solving mass transport or pressure field equations, the computed quantities provide meaningful indicators of curing quality and defect susceptibility.

Conclusions

The results demonstrate that the MFS, when coupled with the MPS–FDM approach, is capable of accurately capturing the transient thermal evolution within the steel–resin domain, even in the presence of a source term in the conduction equation. This highlights its efficiency in reproducing the thermal coupling between layers of dissimilar materials. In addition, the model successfully reproduced both the pressure-evolution curve and the diffusivity $\times$ temperature behavior, showing close agreement with the reference solutions. This indicates that the proposed formulation is not only thermally consistent but also capable of representing the underlying cure-related mass transport phenomena with high fidelity.

However, the deviations observed in Figs. 3 and 4 can be attributed primarily to the inherent difficulty in achieving an optimal calibration of the numerical hyper-parameters. The method's perfor-

mance is strongly influenced by factors such as the number and spatial distribution of collocation and source points, the boundary offset distance, and the Tikhonov regularization parameter. Small variations in these parameters may significantly affect matrix conditioning and solution stability, thereby impacting local accuracy in specific regions of the domain. Thus, although the MFS demonstrates robustness and clear capability in handling non-homogeneous PDEs and coupled multi-physics behavior, the appropriate selection and calibration of hyper-parameters remain central challenges for ensuring both numerical reliability and computational efficiency.

References

[1] Andrea Dei Sommi, Giuseppe Buccoliero, Francesca Lionetto, Fabio De Pascalis, Michele Nacucchi, and Alfonso Maffezzoli. A finite element model for the prediction of porosity in autoclave cured composites. *Composites Part B: Engineering*, 264:110882, September 2023.

[2] Andrea Dei Sommi, Francesca Lionetto, Giuseppe Buccoliero, and Alfonso Maffezzoli. The effect of absorbed moisture and resin pressure on porosity in autoclave cured epoxy resin. *Polymer Composites*, 45(17):15793–15803, August 2024.

[3] Jin-Sang Yoon, Kibum Kim, and Hyoung-Seock Seo. Computational modeling for cure process of carbon epoxy composite block. *Composites Part B: Engineering*, 164:693–702, 2019.

[4] Sandeep Chava and Sirish Namilae. Process modeling for strain evolution during autoclave composite cure. *Applied Composite Materials*, 30(2):361–377, 2023.

[5] B Tomas Johansson and Daniel Lesnic. A method of fundamental solutions for transient heat conduction in layered materials. *Engineering Analysis with Boundary Elements*, 33(12):1362–1367, 2009.

[6] Xin Li. Convergence of the method of fundamental solutions for solving the boundary value problem of modified helmholtz equation. *Applied mathematics and computation*, 159(1):113–125, 2004.

[7] Ching-Shyang Chen, Chia-Ming Fan, and PH Wen. The method of approximate particular solutions for solving certain partial differential equations. *Numerical Methods for Partial Differential Equations*, 28(2):506–522, 2012.

[8] CS Chen, Xinrong Jiang, Wen Chen, and Guangming Yao. Fast solution for solving the modified helmholtz equation withthe method of fundamental solutions. *Communications in Computational Physics*, 17(3):867–886, 2015.

[9] Bandar Bin-Mohsin and Daniel Lesnic. The method of fundamental solutions for helmholtz-type equations in composite materials. *Computers & Mathematics with Applications*, 62(12):4377–4390, 2011.